J. Korean Inst. Electr. Electron. Mater. Eng.
Vol. 38, No. 2, pp. 161-166 March 2025
doi: https://doi.org/10.4313/JKEM.2025.38.2.5
ISSN 1226-7945(Print), 2288-3258(Online)

Regular Paper

Crystallinity and Dielectric Properties for MLCCs According to Heat Treatment of Nano-$BaTiO_3$ Powder Prepared by Hydrothermal Synthesis

Change-Ho Lee and Jung Rag Yoon
R & D Center, Samwha Capacitor, Yongin 17118, Korea

(Received September 30, 2024; Revised October 21 2024; Accepted October 22, 2024)

Abstract: This study examined the crystallinity and potential of $BaTiO_3$ powder, prepared by hydrothermal synthesis at 60 nm, as a dielectric material for automotive MLCCs under varying heat treatment temperatures. At temperatures above 850℃, the powder exhibited an orthorhombic structure, with crystallinity and particle size increasing as the temperature rose. In the range of 850~900℃, the powder displayed a uniform particle size distribution and minimal agglomeration, with particles ranging between 150~200 nm. Additionally, it was confirmed that the heat treatment temperature significantly impacts the properties of $BaTiO_3$ powder, which are critical for the dielectric performance required in X7R MLCCs used in automotive applications. Specifically, high-temperature treatment (above 850℃) was essential for enhancing the powder's crystallinity and forming a stable core-shell structure, which is crucial for achieving stable TCC (Temperature Coefficient of Capacitance) characteristics. It was confirmed that increased crystallinity at temperatures above 850℃ facilitated the development of the core-shell structure through interactions with additives, thereby achieving the necessary characteristics required for highly reliable automotive MLCCs.

Keywords: $BaTiO_3$, MLCC (multilayer ceramic capacitor), Crystallinity, X7R

1. INTRODUCTION

Barium titanate ($BaTiO_3$) is extensively utilized as a fundamental ferroelectric material in a variety of electronic components, such as multilayer ceramic capacitors (MLCCs), due to its superior dielectric and ferroelectric properties. MLCCs are critical passive components in modern electronic devices, and there is a continuous push to reduce the thickness of the dielectric layer to accommodate both the miniaturization and increased capacity requirements of advanced electronic systems. The demand for high-performance and miniaturized electronic components has driven the development of chip components that feature thinner dielectric layers, higher capacity, and enhanced reliability [1-3] This trend necessitates the use of $BaTiO_3$ raw material powders and nanoparticles with a high degree of crystallinity, a stable tetragonal phase, and uniform morphology. It is well established that the crystal structure and dielectric properties of $BaTiO_3$ are significantly influenced by factors such as impurities, defects, particle shape, size, stoichiometry, and homogeneity. These factors largely depend on the manufacturing methods and the specific heat treatment conditions applied during the production process. For MLCCs with high-capacity characteristics, a thin dielectric sheet is required, making high-crystalline, ultra-fine $BaTiO_3$ essential. Methods for producing ultra-fine $BaTiO_3$

✉ **Jung Rag Yoon; yoonjungrag@samwha.com**

powder include the oxalate method, hydrothermal synthesis method, and solid-state method [4-6].

The solid state method has the advantage of high productivity, but has the disadvantages of impurities due to milling and high-temperature calcination processes in the manufacturing process, non-uniformity of particle size and shape, and difficulty in controlling physical and chemical properties. The hydrothermal synthesis method is synthesized through an in-situ reaction mechanism and a dissolution-precipitation reaction mechanism by simultaneously applying temperature and pressure, and can control the particle size, shape, particle size distribution, composition and purity of the ultra-fine $BaTiO_3$ powder. On the other hand, in the case of $BaTiO_3$, a hydrothermal synthesis method, H_2O is formed through a reaction between precursors containing a hydroxy group (-OH, hydroxy group) during the synthesis process, and H_2O escapes from the particles to form pores in the particles [7,8] These intragranular pores reduce the insulation resistance and breakdown voltage of the MLCC, thereby deteriorating the reliability and lifespan characteristics. Due to this, it produces a pseudo-cubic rather than a tetragonal phase due to the OH groups present on the surface and outer layer of the $BaTiO_3$ crystal. $BaTiO_3$ powder manufactured by hydrothermal synthesis is known to be able to control powder size, improve crystallinity, control molar ratio (Ba/Ti), and reduce hydroxy group depending on heat treatment conditions [9]. When $BaTiO_3$ produced by hydrothermal synthesis is sintered in the MLCC manufacturing process, the mobility of pores is low at temperatures below 800℃ and remains in the grains, but at temperatures above 800℃, grain growth is achieved by the Ostwald ripening mechanism and pores in grains is emitted The released pore moves to the vicinity of the MLCC electrode and causes a defect [9]. Due to this, the deterioration of the insulation resistance characteristics of MLCC has been revealed through HALT (highly accelerated life-time test) [10,11]. In this paper, 60 nm-sized $BaTiO_3$ produced through hydrothermal synthesis is studies on the cubic–tetragonal structure transition and microstructure evolution for morphology, BET, particle size in the powder through the heat treatment temperature change. The dielectric and electrical properties suitable for automotive MLCCs with X7R characteristics were investigated using additives to $BaTiO_3$ obtained through heat treatment.

2. EXPERIMENTAL

$BaTiO_3$ powder prepared by hydrothermal synthesis (HBT-006p. Shandong Sinocera Functional Material Co., Ltd., China) was used as a starting material. The characteristics of the $BaTiO_3$ powder used in the experiment were powder size: 60 nm, BET 15.87 (m^2/g), and Ba/Ti molar ratio 1.0008. The start materials were placed in a tube furnace with heat treatment at 200~950℃ for 2 h under atmosphere and then cooled down to ambient temperature in the furnace. To evaluate the potential of heat-treated $BaTiO_3$ as a raw material for MLCCs with X7R temperature characteristics (capacitance change within ±15% over a range of -55℃ to 125℃), an experiment was conducted by adding MgO, Mn_3O_4, V_2O_5, and rare earth elements to the heat-treated $BaTiO_3$. After the additives were incorporated into the heat-treated $BaTiO_3$, wet mixing and milling were performed using a nano mill with 0.1 mm spherical zirconia balls and an ethanol/toluene mixture. The resulting mixed powder was used to prepare a slurry with PVB, ethanol, and toluene, which was then used to produce green sheets via the doctor blade method. The green sheets were laminated, pressed, and cut to produce chips. After binder removal, the chips were sintered for 2 hours at 1,160~1,220℃ in a reducing atmosphere (with an oxygen partial pressure of 10^{-11}~10^{-13} atm), and silver electrodes were formed on both sides to create samples for dielectric property measurement. The heat-treated powders at various temperatures were analyzed using a laser diffraction particle size analyzer (LA960V2, HORIBA, JAPAN), and the microstructure was observed using a field emission electron microscope (FESEM, JSM-9701, JEOL, JAPAN). The thermal behaviours of the heat-treated powders were evaluated using a thermogravimetric analysis (SDT Q600, TA instruments) in the range of 40~1,100℃ at 10℃/min. The crystalline structure of $BaTiO_3$ powder were determined using an X-ray diffractometer (XRD) (BRUKER AXS D4 ENDEAVOR) with Cu–Kα radiation. The morphologies and sizes of the $BaTiO_3$ powders were analyzed using a field-emission scanning electron microscope, The dielectric properties of the samples were measured using an LCR meter (HP 4284A at 1.0 kHz and 1.0 Vrms to determine the dielectric constant and quality factor. Insulation resistance was measured using a high resistance meter (HP 4339B) after applying 100 V for 60 seconds. The temperature coefficient of

capacitance (TCC) was measured from -55℃ to 125℃ under temperature conditions at a measurement frequency of 1 kHz using an LCR meter (HP 4284A) in a temperature chamber.

3. RESULTS AND DISCUSSION

Figure 1 shows the thermo gravimetric analysis (TGA) results of $BaTiO_3$ powders synthesized by the hydrothermal method and subjected to heat treatments at 200℃ and 900℃. The TGA data demonstrate weight loss across three distinct temperature ranges. In the range of 25℃ to 200℃, the weight loss is primarily due to the evaporation of solvents or moisture used during the hydrothermal synthesis process. Between 200℃ and 360℃, the weight loss occurs due to the decomposition of hydroxyl groups (-OH) formed during synthesis, resulting in the release of water vapor and other volatile substances. In the 380℃ to 1,100℃ range, the weight loss is mainly attributed to the decomposition of organic materials and the removal of bound water, which are associated with the formation of the $BaTiO_3$ crystalline structure. At temperatures above 850℃, the weight loss of the powders is less than 0.6%, indicating that the $BaTiO_3$ has fully transitioned into a stable crystalline structure and achieved thermal stability.

Figure 2 shows the XRD results of $BaTiO_3$ powder synthesized by the hydrothermal method and subsequently heat-treated at temperatures ranging from 200℃ to 900℃. The powder heat-treated below 800℃ exhibits a cubic structure, while the powder heat-treated above 850℃ shows a tetragonal structure, with a noticeable decrease in the full width at half maximum (FWHM). In the XRD pattern, within the 2θ range of 44° to 46°, it is observed that, starting from temperatures above 850℃, the peaks split into two distinct peaks corresponding to the (002) and (200) planes. As the heat treatment temperature increases, this separation becomes more pronounced. These results indicate that the $BaTiO_3$ particles, initially synthesized in the cubic phase, undergo a phase transformation to the tetragonal phase.

Figure 3 presents the results of crystallinity and cell volume as a function of heat treatment temperature, defining the ratio of the lattice constants (c/a) for the (002) and (200) planes as the tetragonality of the $BaTiO_3$ particles. Up to 800℃, $BaTiO_3$ crystallizes in a cubic structure, starting with a crystallinity of 1.0. As the temperature increases, the tetragonality (c/a) also increases due to the elongation of the C-axis. At 850℃, the c/a ratio reaches 1.006, and at 900℃, it further increases to 1.01, indicating a high degree of crystallinity. Generally, the crystallinity of $BaTiO_3$ is known to be closely related to the particle size and density, with higher crystallinity being advantageous for the long-term lifespan characteristics of MLCCs [12].

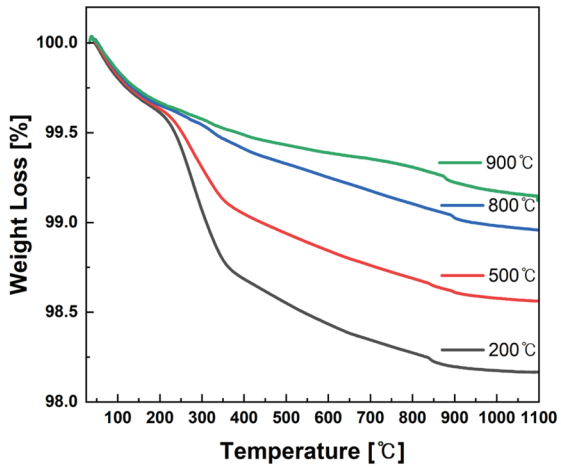

Fig. 1. TGA curves of hydrothermally synthesized nano $BaTiO_3$ powders at various heat treatment temperature.

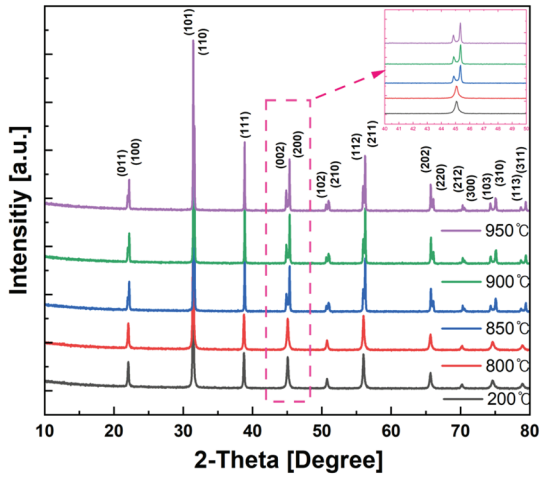

Fig. 2. XRD patterns of hydrothermally synthesized nano $BaTiO_3$ powders at heat treatment temperature.

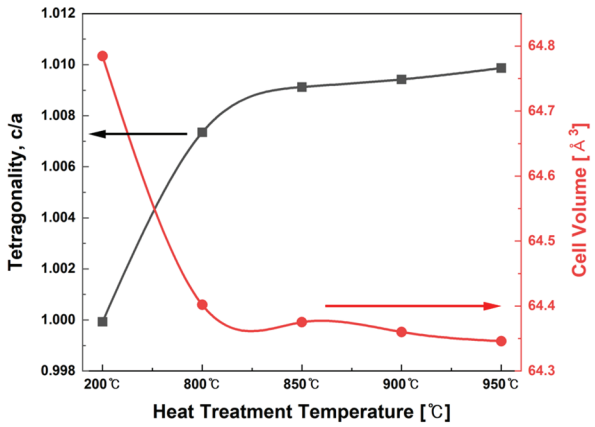

Fig. 3. Tetragonality and cell volume of hydrothermally synthesized nano $BaTiO_3$ powders at various heat treatment temperature.

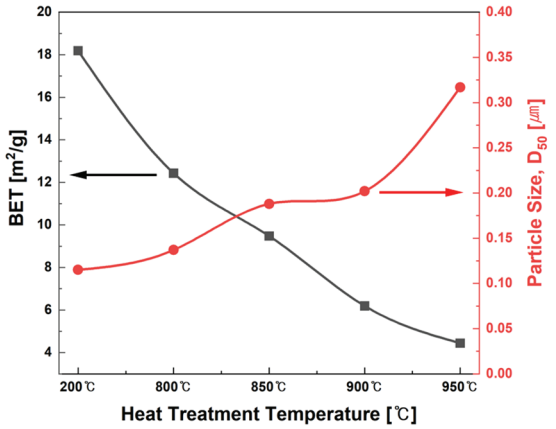

Fig. 4. BET and particle size of hydrothermally synthesized nano $BaTiO_3$ powders at various heat treatment temperature.

Figure 4 shows the results of measuring the specific surface area and particle size (D_{50}) of powder produced by the hydrothermal synthesis method as a function of the heat treatment temperature. As the heat treatment temperature increases, the specific surface area decreases from 18 m^2/g to 3.8 m^2/g, while the particle size (D_{50}) increases from 80 nm to 180 nm. This result can be attributed to the fact that, at higher temperatures, particles agglomerate or crystal growth occurs, strengthening the interparticle bonds. Additionally, the removal of impurities (e.g., -OH) from the powder surface and the alignment of the crystal structure can lead to the formation of new surfaces or a reduction in surface defects, resulting in a decreased specific surface area [13,14]. The particle size distribution can show a decreasing trend in the average particle size (D_{50}) as the calcination temperature increases, due to the increased thermal energy, which causes particles to bind more strongly, leading to more uniform particle sizes and increased density.

Figure 5 shows the microstructure of the powder according to the heat treatment temperature. The $BaTiO_3$ powder heat-treated at 800°C is in the early stages of grain growth, with individual particles not sufficiently grown and existing in an agglomerate form similar to the initial raw material. As the heat treatment temperature increases to 850°C and 900°C, particle agglomeration decreases, and the powder shows a mono dispersed form suitable for high-capacity MLCC manufacturing. The $BaTiO_3$ particles grow in a shape close to spherical, with the grain growth and minimization of surface energy, resulting in a smoother and more uniform particle

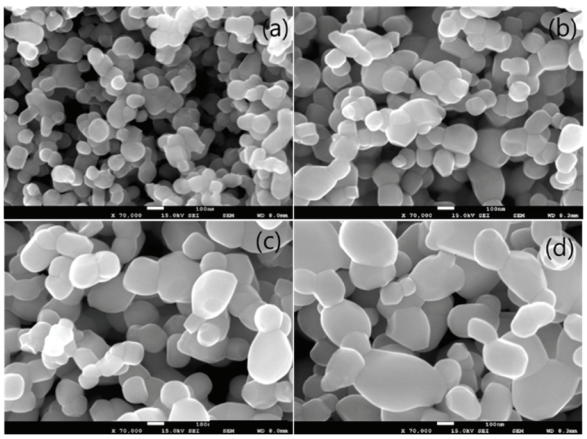

Fig. 5. SEM hydrothermally synthesized nano $BaTiO_3$ powders at various heat treatment temperature: (a) 800°C, (b) 850°C, (c) 900°C, and (d) 950°C.

surface. However, at 950°C, the heat treatment promotes bonding between particles, leading to the formation of 'peanut-shaped' agglomerates and a tendency to form irregular agglomerate structures. This microstructure is considered unsuitable for use as a raw material for high-capacity MLCCs.

Figure 6 illustrates the dielectric constant and loss characteristics of samples sintered at 1,160~1,220°C, composed of $BaTiO_3$ powder with added MgO, Mn_3O_4, V_2O_5, and rare earth elements, according to the heat treatment temperature. The $BaTiO_3$ powder heat-treated at 800°C was sintered at 1,160°C, and as the heat treatment temperature increased, the sintering temperature was raised to 1,220°C. The dielectric constant is observed to increase as the heat

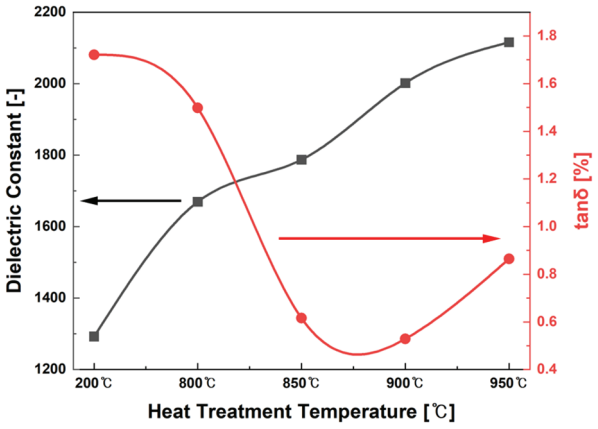

Fig. 6. Dielectric constant and dielectric loss according to $BaTiO_3$ powders at various heat treatment temperature.

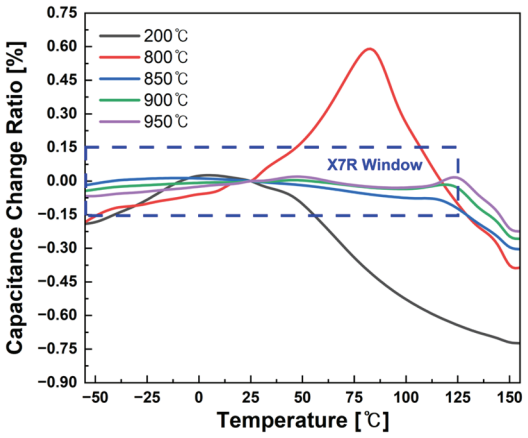

Fig. 7. TCC according to $BaTiO_3$ powders at various heat treatment temperature.

treatment temperature rises. This result can be attributed to the fact that $BaTiO_3$ powder with higher crystallinity has fewer structural defects, and as crystallinity increases, the degree of polarization improves, leading to a higher dielectric constant. Dielectric loss is known to be influenced by the crystal structure and secondary phases, with impurities and defects at the grain boundaries being a major cause of electrical loss. Up to around 900°C, the increase in particle size leads to a reduction in the number of grain boundaries, which is believed to be the reason for the observed results [15-17].

Figure 7 illustrates the TCC of samples sintered at 1,160~1,220°C, composed of $BaTiO_3$ powder with added MgO, Mn_3O_4, V_2O_5, and rare earth elements, according to the heat treatment temperature. In high-capacity BME MLCCs, the TCC characteristics of the X7R grade are known to arise from the core-shell grain structure, where the core is composed of pure $BaTiO_3$, and the shell is formed by the diffusion of additives into $BaTiO_3$. For X7R-grade MLCCs, the capacitance change (TCC) with temperature must be limited to within ±15%, which is significantly influenced by the microstructure of $BaTiO_3$, particularly the core-shell structure. The core consists of pure $BaTiO_3$, while the shell is a structure formed by the diffusion of additives, providing stability to the dielectric properties against temperature changes. $BaTiO_3$ powder heat-treated at 200°C exhibited low crystallinity and small particle size, which were insufficient to achieve adequate sinterability, thereby hindering the formation of the core-shell structure. As a result, it was challenging to achieve a flattened temperature characteristic attributed to the core-shell structure, and the TCC characteristics were unsuitable as a dielectric material for high-capacity X7R MLCCs. The cubic structure of $BaTiO_3$ powder heat-treated at 800°C showed some characteristics of a core-shell structure, but it was significantly affected by the formation of new crystal phases that exhibited effects such as shifters and depressers [18-21].

4. CONCLUSION

This study investigated the crystallinity and characteristics of $BaTiO_3$ powder prepared by hydrothermal synthesis at various heat treatment temperatures. The powder exhibited an orthorhombic structure at temperatures above 850°C, and the crystallinity and particle size increased with rising temperatures. In the temperature range of 850~900°C, the powder showed excellent surface uniformity with minimal agglomeration, producing particles in the range of 150~200 nm, which are suitable for the manufacture of high-capacity X7R MLCCs. Furthermore, it was confirmed that the heat treatment temperature plays a critical role in determining the dielectric properties for achieving X7R characteristics in high-capacity BME MLCCs. In particular, high-temperature treatments (above 850°C) were essential for enhancing the crystallinity of the powder and forming a stable core-shell structure, which is crucial for achieving stable TCC characteristics. These findings provide important guidelines for establishing appropriate heat treatment conditions in the manufacturing process of high-performance MLCCs. At

temperatures above 850℃, the crystallinity of the $BaTiO_3$ powder became more pronounced, leading to the formation of a core-shell structure due to its interaction with the additives. As a result, samples treated at high temperatures were found to meet the TCC characteristics required for X7R automotive MLCCs grade materials.

ORCID

Jung Rag Yoon https://orcid.org/0000-0002-9206-8701

ACKNOWLEDGMENTS

This work was supported by the Technology Innovation Program (RS-2024-00430833, Development of MLCC commercialization technology for automotive electronics an alternative to rare earth for high reliability response) funded by the Ministry of Trade, Industry & Energy (MOTIE, Korea).

REFERENCES

[1] K. Hong, T. H. Lee, J. M. Suh, S. H. Yoon, and H. W. Jang, *J. Mater. Chem. C*, **7**, 9782 (2019).
doi: https://doi.org/10.1039/c9tc02921d

[2] H. Song, G. Lee, J. Ye, J. Y. Jung, D. Y. Jeong, and J. Ryu, *J. Korean Inst. Electr. Electron. Mater. Eng.*, **37**, 119 (2024).
doi: https://doi.org/10.4313/JKEM.2024.37.2.1

[3] C. H. Lee and J. R. Yoon, *J. Ceram. Process. Res.*, **24**, 588 (2023).
doi: https://doi.org/10.36410/jcpr.2023.24.3.588

[4] G. Pfaff, *J. Mater. Chem.*, **2**, 591 (1992).
doi: https://doi.org/10.1039/jm9920200591

[5] C. T. Xia, E. W. Shi, W. Z. Zhong, and J. K. Guo, *J. Eur. Ceram. Soc.*, **15**, 1171 (1995).
doi: https://doi.org/10.1016/0955-2219(95)00101-8

[6] H. T. Kim, J. H. Kim, W. S. Jung, and D. H. Yoon, *J. Ceram. Process. Res.*, **10**, 753 (2009).

[7] Y. J. Kim, M. H. Choi, H. S. Shin, B. K. Ju, and M. P. Chun, *J. Korean Inst. Electr. Electron. Mater. Eng.*, **33**, 483 (2020).
doi: https://doi.org/10.4313/JKEM.2020.33.6.483

[8] J. Lee, H, Jeong, and S. Ma, *Mater. Res. Express*, **9**, 065001 (2022).
doi: https://doi.org/10.1088/2053-1591/ac73e2

[9] M. T. Buscaglia, N. Bassoli, V. Buscaglia, and R. Vormberg, *J. Am. Ceram. Soc.*, **91**, 2862 (2008).
doi: https://doi.org/10.1111/j.1551-2916.2008.02576.x

[10] J. Li, K. Inukai, A. Tsuruta, Y. Takahashi, and W. Shin, *J. Asian Ceram. Soc.*, **5**, 444 (2017).
doi: https://doi.org/10.1016/j.jascer.2017.09.006

[11] J. Kim, S. H. Lee, J. R. Yoon, C. J. Van Tyne, K. Y. Ohk, and H. Lee, *J. Test. Eval.*, **44**, 1593 (2016).
doi: https://doi.org/10.1520/jte20140522

[12] C. Pithan, D. Hennings, and R. Waser, *Int. J. Appl. Ceram. Technol.*, **2**, 1 (2005).
doi: https://doi.org/10.1111/j.1744-7402.2005.02008.x

[13] H. Hayashi and Takeo Ebina, *J. Ceram. Soc. Jpn.*, **126**, 214 (2018).
doi: https://doi.org/10.2109/jcersj2.17125

[14] H. S. Lee and J. R. Yoon, *J. Korean Inst. Electr. Electron. Mater. Eng.*, **37**, 662 (2024)
doi: https://doi.org/10.4313/JKEM.2024.37.6.13

[15] S. H. Yoon, S. J. Kim, S. H. Kim, and D. Y. Kim, *J. Appl. Phys.*, **114**, 224103 (2013).
doi: https://doi.org/10.1063/1.4844575

[16] L. Zhang and X. Wang, *J. Adv. Ceram.*, **9**, 234 (2020).

[17] S. H. Kim, et al., *Mater. Sci. Eng., B*, **245**, 65 (2019).

[18] Q. Li, T. Ju, R. Li, S. Wang, Y. Yang, H. Ishida, Y. W. Harn, J. Chen, B. Hirt, A. Sehirlioglu, Z. Lin, and L. Zhu, *Nanoscale*, **15**, 7829 (2023).
doi: https://doi.org/10.1039/d3nr00350g

[19] V. Buscaglia and C. A. Randall, *J. Eur. Ceram. Soc.*, **40**, 3744 (2020).
doi: https://doi.org/10.1016/j.jeurceramsoc.2020.01.021

[20] V. Buscaglia, M. T. Buscaglia, M. Viviani, L. Mitoseriu, P. Nanni, V. Trefiletti, P. Piaggio, I. Gregora, T. Ostapchuk, J. Pokorný, and J. Petzelt, *J. Eur. Ceram. Soc.*, **26**, 2889 (2006).
doi: https://doi.org/10.1016/j.jeurceramsoc.2006.02.005

[21] J. R. Yoon and M. K. Kim, *J. Electr. Eng. Technol.*, **15**, 2685 (2020).
doi: https://doi.org/10.1007/s42835-020-00505-7